Phase diagram of the extended Hubbard model in one spatial dimension

Joel W. Cannon and Eduardo Fradkin
Department of Physics, Univeristy of Illinois at Urbana–Champaign, 110 West Green Street, Urbana, Illinois 61801
(Received 18 January 1989)

We report results obtained for the phase diagram and critical behavior of the extended Hubbard model in one spatial dimension at half-filling. We show that umklapp scattering is responsible for the tricritical behavior. We calculate the critical exponents at the tricritical point, and along the critical line separating the charge- and spin-density-wave phases. In addition, using Monte Carlo simulations we estimate the position of the tricritical point to occur at approximately $U=1.5$ and $V=3.1$ in units of the hopping energy.

I. INTRODUCTION

The extended Hubbard model is a simple many-body model which has a rich phase structure. It consists of spin-$\frac{1}{2}$ fermions which may hop between sites on a lattice, and which interact with each other via an on-site and nearest-neighbor potentials. It is given by the Hamiltonian

$$H=-t\sum_{i,\sigma}(C^{\dagger}_{i,\sigma}C_{i+1,\sigma}+C^{\dagger}_{i+1,\sigma}C_{i,\sigma}) +U\sum_i n_{i\uparrow}n_{i\downarrow}+V\sum_i n_i n_{i+1}\,, \qquad n_i=n_{i\uparrow}+n_{i\downarrow}\,. \tag{1}$$

Here $C^{\dagger}_{i,\sigma}$ and $C_{i,\sigma}$ are the creation and annihilation operators for a fermion of spin σ at the ith spatial site, $n_{i,\sigma}=C_{i,\sigma}C^{\dagger}_{i,\sigma}$ is the number operator, U is the on-site interaction strength, V is the nearest-neighbor interaction strength, and t is the hopping strength.

We are interested in the half-filled band case, with $U,V>0$. This has two ordered phases, a charge-density-wave (CDW), and a spin-density-wave (SDW) phase. The CDW phase has a discrete symmetry, and exhibits true long-range order, while the SDW phase has a continuous symmetry, and consequently, by the Mermin-Wagner theorem, cannot have true long-range order. Rather, it is a critical state in the sense that the staggered spin-density correlation function decays slowly (algebraically). The important questions concerning the model are as follows: Where is the boundary between the two phases located, and what is the nature of the transition between the two phases?

Until recently, the phase boundary was thought to occur at $U=2V$ for all values of U, and to be first order. Weak-coupling renormalization-group (RG) calculations[1] and Hartree-Fock calculations[2] give the same $U=2V$ boundary obtained by strong-coupling arguments. It seemed likely, therefore, that this same boundary would occur for intermediate values of the coupling constants as well. Callen and Cabib also deduced from the Hartree-Fock calculations that the transition was first order. Their calculations gave three solutions at the $U=2V$ line: a mixed phase, and pure CDW and SDW phases. The CDW and SDW states were found to have lower energies than the mixed phase, leading to the conclusion that the transition in crossing the boundary was discontinuous, or first order.

In 1984, Fourcade and Spronken[3,4] calculated the phase diagram using a block-spin RG, and a type of finite-sized scaling developed by Sneddon,[5] and found that the phase boundary was shifted in the direction of the CDW region as shown in Fig. 1, and that the phase transition is second order. In retrospect, it is not clear whether their RG was capable of observing a first-order transition since they made no provisions in the renormalized Hamiltonian for the generation of terms differing in symmetry from the original terms. Failure to do this when performing RG analysis on the Potts model made it impossible to find a first-order transition where one was known to exist.[6] In addition, the umklapp scattering terms, which we find to be important, were absent from the Hamiltonian used in the finite-sized scaling.[4]

Monte Carlo calculations performed by Hirsch[7,8] confirmed the shift in the phase boundary but found that the transition was second order for small values of the coupling constant, and first order for large values. Hirsch estimated the tricritical point to be approximately $U=3.0$. In addition, he presented a qualitative argument for the presence of the tricritical point, using the concept of droplets of either CDW or SDW phases, and a strong coupling analytical calculation for the shifted phase boundary using the Bethe ansatz. A further conjecture was that the tricritical point was associated with the essential singularity of a Kosterlitz-Thouless transition.

In this paper, we present analytic results that reveal the physics responsible for the tricritical point, and numerical calculations that more accurately locate its position. We first consider the continuum limit of the theory, showing that the transition between the CDW and SDW phases indeed changes from second order to first order due to the role of an umklapp scattering term, which becomes relevant at higher values of the coupling constants. Since the theory contains only sine-Gordon-type operators, it also confirms that the first-order transition appears with an essential singularity. In addition, we present the results of some detailed Monte Carlo calculations which confirm the change from a second- to first-order transition at a value of approximately $U=1.5$.

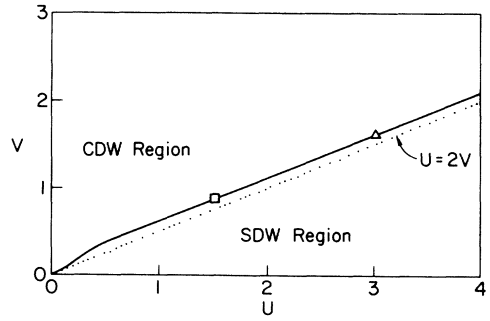

FIG. 1. Qualitative plot showing the phase diagram of the extended Hubbard model at half-filling. Note that the CDW-SDW boundary occurs at values of $V > U/2$. We find that the transition is first order above approximately $U=1.5$ (indicated by the square). Hirsch earlier found it to be first order above approximately $U=3.0$ (indicated by the triangle).

II. RESULTS IN THE CONTINUUM LIMIT

The physics behind the extended Hubbard model becomes more transparent if we transform to k space and consider the operators involved in the various scattering processes (channels). In the continuum limit the kinetic-energy part of the Hamiltonian can be written

$$H_0=-\left[\frac{L}{2\pi}\right]\int_{-\pi/2}^{\pi/2}dq\,E(q)(\psi_{R,\sigma}^{\dagger}\psi_{R,\sigma}-\psi_{L,\sigma}^{\dagger}\psi_{L,\sigma})\ , \tag{2}$$

$$\frac{L}{2\pi}\int_{-\pi/2}^{\pi/2}dq\,\psi_{R,\sigma}(q)=\frac{L}{2\pi}\int_{0}^{\pi}dk\,\psi_{\sigma}(k)\ , \tag{3}$$

$$=\lim_{L\to\infty}\frac{1}{L}\sum_{k>0}C_{k,\sigma}\ , \tag{4}$$

$$\frac{L}{2\pi}\int_{-\pi/2}^{\pi/2}dq\,\psi_{L,\sigma}(q)=\frac{L}{2\pi}\int_{-\pi}^{0}dk\,\psi_{\sigma}(k)\ , \tag{5}$$

$$=\lim_{L\to\infty}\frac{1}{L}\sum_{k<0}C_{k,\sigma}\ , \tag{6}$$

$$E(q)=2t\sin(q)\ , \tag{7}$$

$$\approx v_f q\ , \tag{8}$$

$$v_f=2t\ . \tag{9}$$

ψ_L and ψ_R represent "left" and "right" moving fermions, and are the components of a spinor. Using this fact, the equation can be compactly expressed in Dirac notation:

$$H=-\left[\frac{L}{2\pi}\right]\int_{-\pi/2}^{\pi/2}dq\,E(q)\psi^{\dagger}\gamma_5\psi\ , \tag{10}$$

$$\approx v_f\int dx\,(-i)\psi^{\dagger}\gamma_5\frac{\partial}{\partial x}\psi\ , \tag{11}$$

$$\gamma_5=\sigma_3=\begin{bmatrix}1&0\\0&-1\end{bmatrix}\ ,$$

$$\psi=\sigma\begin{bmatrix}\psi_{R,\sigma}\\ \psi_{L,\sigma}\end{bmatrix}\ .$$

In these last equations, we have assumeed that all relevant physics occurs near the Fermi surface (i.e., points $k=\pm\pi/2$), and have linearized the energy spectrum about these points. Since we have linearized the spectrum, $E(q)=2tq=v_f q$. Written in this manner, it is apparent that this is a system of relativistic fermions where the velocity of light is the Fermi velocity (for another example of this technique, see Ref. 1).

We now transform the on-site interaction term into a basis of left and right movers to obtain

$$\begin{aligned}H_U=-&\left[\frac{L}{2\pi}\right]\int_{-\pi/2}^{\pi/2}\left[\frac{dq_1}{2\pi}\right]\left[\frac{dq_2}{2\pi}\right]\left[\frac{dq_3}{2\pi}\right]\left[\frac{dq_4}{2\pi}\right]\\
&\times[\psi_{R,\uparrow}^{\dagger}(q_1)\psi_{R,\uparrow}(q_2)\psi_{R,\downarrow}^{\dagger}(q_3)\psi_{R,\downarrow}(q_4)+\psi_{L,\uparrow}^{\dagger}(q_1)\psi_{L,\uparrow}(q_2)\psi_{L,\downarrow}^{\dagger}(q_3)\psi_{L,\downarrow}(q_4)\\
&+\psi_{L,\uparrow}^{\dagger}(q_1)\psi_{L,\uparrow}(q_2)\psi_{R,\downarrow}^{\dagger}(q_3)\psi_{R,\downarrow}(q_4)+\psi_{R,\uparrow}^{\dagger}(q_1)\psi_{R,\uparrow}(q_2)\psi_{L,\downarrow}^{\dagger}(q_3)\psi_{L,\downarrow}(q_4)]\delta(q_1+q_2-q_3-q_4)\\
&+[\psi_{L,\uparrow}^{\dagger}(q_1)\psi_{R,\uparrow}(q_2)\psi_{L,\downarrow}^{\dagger}(q_3)\psi_{R,\downarrow}(q_4)+\psi_{R,\uparrow}^{\dagger}(q_1)\psi_{R,\downarrow}(q_2)\psi_{L,\downarrow}^{\dagger}(q_3)\psi_{L,\uparrow}(q_4)\\
&+\psi_{L,\uparrow}^{\dagger}(q_1)\psi_{R,\uparrow}(q_2)\psi_{L,\downarrow}^{\dagger}(q_3)\psi_{R,\downarrow}(q_4)+\psi_{R,\uparrow}^{\dagger}(q_1)\psi_{L,\uparrow}(q_2)\psi_{R,\downarrow}^{\dagger}(q_3)\psi_{L,\downarrow}(q_4)]\delta(q_1+q_2-q_3-q_4-2\pi)\ .\end{aligned} \tag{12}$$

We see that the on-site interaction actually contains eight scattering terms including forward, back, and umklapp processes. These are shown in Fig. 2. The forward and backscattering terms are invariant under a continuous chiral transformation $\psi'_{\sigma}=e^{i\gamma_5\theta}\psi_{\sigma}$. However, the umklapp terms have only a discrete chiral symmetry. Thus, the umklapp term is responsible for a discrete symmetry in the model which can be broken when the system undergoes a phase transition.

We can express the on-site interaction more compactly if we define the currents

$$J_{\mu}=\bar{\psi}\gamma_{\mu}\psi\ , \tag{13}$$

$$J_{\mu}^{3}=\bar{\psi}\gamma_{\mu}\tau_3\psi\ , \tag{14}$$

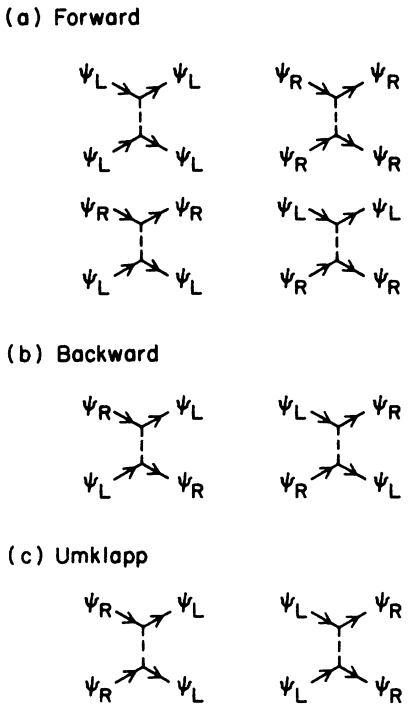

FIG. 2. Classification of scattering processes found when interaction terms are expressed in a basis of left and right moving fermions.

$$\bar{\psi}=\sum_{\sigma}\psi_{\sigma}^{\dagger}\gamma_0 , \tag{15}$$

$$\tau_3=\sigma_3 . \tag{16}$$

In these definitions, the γ matrices operate on the left and right components of ψ, and the matrix τ_3 operates on the spin components. Thus

$$\tfrac{1}{2}(J_0+J_0^3)=\psi_{L,\uparrow}^{\dagger}\psi_{L,\uparrow}+\psi_{R,\uparrow}^{\dagger}\psi_{R,\uparrow} , \tag{17}$$

$$\tfrac{1}{2}(J_0-J_0^3)=\psi_{L,\downarrow}^{\dagger}\psi_{L,\downarrow}+\psi_{R,\downarrow}^{\dagger}\psi_{R,\downarrow} . \tag{18}$$

Using these definitions, the on-site term reduces to

$$H_U=-\frac{U}{4}\int dx\,[J_0^2-(J_0^3)^2+(\bar{\psi}\psi)^2-(\bar{\psi}\tau_3\psi)^2] . \tag{19}$$

Finally, the nearest-neighbor term can be written

$$H_V=-V\int dx\left[\sum_{\sigma}\psi_{\sigma}^{\dagger}\psi_{\sigma}\right]^2-V\int dx\left[\sum_{\sigma}\bar{\psi}_{\sigma}\psi_{\sigma}\right]^2 . \tag{20}$$

Combining these terms the full Hamiltonian can be written

$$H_{\rm tot}=v_f\int dx\,(-i)\psi^{\dagger}\gamma_5\frac{\partial}{\partial x}\psi + \int dx\left[\left[\frac{U}{4}+\frac{V}{2}\right]J_0^2+\left[\frac{U}{4}-\frac{V}{2}\right](\bar{\psi}\psi)^2 + \frac{U}{4}(J_0^3)^2-\frac{U}{4}(\bar{\psi}\tau_3\psi)^2\right] . \tag{21}$$

This is equivalent to the Lagrangian.

$$L=\bar{\psi}_s i\partial\!\!\!/\psi_s-\left[\frac{U}{8}+\frac{V}{2}\right](\bar{\psi}_s\gamma_0\psi_s)^2 + \left[\frac{V}{2}-\frac{U}{8}\right](\bar{\psi}_s\psi_s)^2 + \frac{U}{8}(\bar{\psi}_s\gamma_0\tau_3\psi_s)^2+\frac{U}{8}(\bar{\psi}_s\tau_3\psi_s)^2 . \tag{22}$$

In the last equation, the lengths have been rescaled to make $v_f=1$, and the coupling constants are expressed in units of t. To proceed further, we convert from Fermi to Bose fields. From the work of Mandelstam[9] and Witten,[10] we obtain the following identities which relate the Fermi fields, ψ, to Bose fields, ϕ:

$$\bar{\psi}_s i\partial\!\!\!/\psi_s=\tfrac{1}{2}(\partial_\mu\phi_s)^2 , \tag{23}$$

$$\bar{\psi}_s\psi_s=\frac{1}{\pi a_0}:\cos(\sqrt{4\pi}\phi_s): \tag{24}$$

$$\bar{\psi}_s\gamma_\mu\gamma_s=\frac{1}{\sqrt{\pi}}\epsilon_{\mu\nu}\partial^{\nu}\phi_s , \tag{25}$$

$$\bar{\psi}_s\tau_3\psi_s=\frac{1}{\pi a_0}[:\cos(\sqrt{4\pi}\phi_\uparrow):-:\cos(\sqrt{4\pi}\phi_\downarrow):] \tag{26}$$

$$\bar{\psi}_s\gamma_\mu\tau_3\psi_s=\frac{1}{\sqrt{\pi}}\epsilon_{\mu\nu}\partial^{\nu}(\phi_\uparrow-\phi_\downarrow) . \tag{27}$$

In addition to transforming to Bose fields, we have introduced a short distance cutoff a_0. In what follows, the normal ordering symbol, ::, will be suppressed, but normal ordering will be implicit in all equations.

Using these identities, we express the Lagrangian as

$$L=\frac{1}{2}\sum_s(\partial_\mu\phi_s)^2-\left[\frac{U}{4}+V\right]\frac{1}{2\pi}\sum_s(\partial_1\phi_s)+\frac{U}{8\pi}(\partial_1\phi_\uparrow-\partial_1\phi_\downarrow)^2 + \left[V-\frac{U}{2}\right]\frac{1}{a_0^2\pi^2}\cos(\sqrt{4\pi}\phi_\uparrow)\cos(\sqrt{4\pi}\phi_\downarrow)+\frac{V}{4\pi^2a_0^2}[\cos(\sqrt{4\pi}\phi_\uparrow)+\cos(\sqrt{4\pi}\phi_\downarrow)]+\frac{2V}{\pi}\sum_s(\partial_\mu\phi_s)^2 . \tag{28}$$

In this last equation we have also used the operator product expansion

$$\frac{1}{a_0^2}\sum_s \cos^2(\sqrt{4\pi}\phi_s)=\frac{1}{2a_0^2}\sum_s \cos(\sqrt{4\pi}\phi_s) + \text{const} + \frac{\pi}{2}\sum_s (\partial_\mu \phi_s)^2 . \quad (29)$$

The lattice Hamiltonian for the extended Hubbard model has now been converted to a continuum Lagrangian field theory containing only sine-Gordon-type Bose operators. Our strategy is now to separate the CDW and SDW degrees of freedom, rescale the lengths and fields to obtain a more standard form, and read off the scaling dimensions of the operators in terms of the coupling constants U and V. Along the naive phase boundary $U=2V$, we will find that one of the operators is irrelevant at small values of the coupling constants, but becomes relevant at larger values. In the standard terminology, this opens up a gap between the two phases, signaling a change in the transition from second to first order.

We begin by separating the charge- and spin-density-wave degrees of freedom. Because the theory was constructed by linearizing about the Fermi points $K_f=\pm\pi/2$, both charge and spin degrees of freedom refer to waves of period twice that of the lattice constant.

$$\frac{1}{\sqrt{2}}(\phi_\uparrow+\phi_\downarrow)=\phi_{\text{CDW}} , \quad (30)$$

$$\frac{1}{\sqrt{2}}(\phi_\uparrow-\phi_\downarrow)=\phi_{\text{SDW}} , \quad (31)$$

$$L=\left[1+\frac{4V}{\pi}\right]\frac{1}{2}\sum_s (\partial_\mu\phi_s)^2-\left[\frac{U}{4}+V\right]\frac{1}{\pi}(\partial_1\phi_{\text{CDW}})^2 + \frac{U}{4\pi}(\partial_1\phi_{\text{SDW}})^2+\left[V-\frac{U}{2}\right]\frac{1}{2a_0^2} \times[\cos(\sqrt{8\pi}\phi_{\text{CDW}})+\cos(\sqrt{8\pi}\phi_{\text{SDW}})]^2 + \frac{V}{4\pi^2 a^2}\{\cos[\sqrt{4\pi}(\phi_{\text{CDW}}+\phi_{\text{SDW}})] + \cos[\sqrt{4\pi}(\phi_{\text{CDW}}-\phi_{\text{SDW}})]\} . \quad (32)$$

Next, we rescale the lengths and fields:

$$\phi_\nu=\mu_\nu\xi_{n u} , \quad (33)$$

$$x_0=z_0 , \quad (34)$$

$$x_1=bz_1 , \quad (35)$$

$$\beta_{\text{CDW,SDW}}=\sqrt{8\pi}(\mu_{\text{CDW,SDW}}) . \quad (36)$$

Using these definitions, the Lagrangian becomes

$$L=\sum_\nu \Gamma_{0\frac{1}{2}}^{\nu}(\partial_0\xi_\nu)^2-\Gamma_1^{\text{CDW}}(\partial_1\xi_{\text{CDW}})^2 - \Gamma_1^{\text{SDW}}(\partial_1\xi_{\text{SDW}})^2+\frac{G_2}{a_0^2}\sum_\nu \cos(\beta_\nu\xi_\nu) + \frac{G_1}{2a_0^2}\cos(\beta_{\text{CDW}}\xi_{\text{CDW}})\cos(\beta_{\text{SDW}}\xi_{\text{SDW}}) , \quad (37)$$

$$G_1=\frac{Vb}{2\pi_2} , \quad (38)$$

$$G_2=\left[V-\frac{U}{2}\right]\frac{b}{2\pi} , \quad (39)$$

$$\Gamma_0^{\text{CDW}}=b\mu_{\text{CDW}}^2\left[1+\frac{4V}{\pi}\right] , \quad (40)$$

$$\Gamma_0^{\text{SDW}}=b\mu_{\text{SDW}}^2\left[1+\frac{4V}{\pi}\right] , \quad (41)$$

$$\Gamma_1^{\text{CDW}}=\frac{\mu_{\text{CDW}}^2}{b}\left[1+\frac{12V+U}{2\pi}\right] , \quad (42)$$

$$\Gamma_1^{\text{SDW}}=\frac{\mu_{\text{SDW}}^2}{b}\left[1+\frac{8V+U}{2\pi}\right] . \quad (43)$$

We now have four normalization constants which are functions of the three arbitrary constants we have introduced in rescaling lengths and fields, and the coupling constants U and V. Since we are free to choose the normalization constants, we set $\Gamma_0^{\text{CDW}}=\Gamma_1^{\text{CDW}}=1$, giving

$$b=\left[\frac{1+(12V+U)/2\pi}{v_f+8V/2\pi}\right]^{1/2} , \quad (44)$$

$$\mu_{\text{CDW}}^2=\left[1+\frac{12V+U}{2\pi}\right]^{-1/2}\left[1+\frac{8V}{2\pi}\right]^{-1/2} . \quad (45)$$

Next, we parametrize the SDW constants

$$\Gamma_0^{\text{SDW}}=\eta^2 , \quad (46)$$

$$\Gamma_1^{\text{SDW}}=\frac{1}{\eta^2} . \quad (47)$$

This gives

$$\mu_{\text{SDW}}^2=\left[1+\frac{8V-U}{2\pi}\right]^{-1/2}\left[1+\frac{8V}{2\pi}\right]^{-1/2} , \quad (48)$$

$$\eta^2=\frac{(1+8V/2\pi)^{-1/2}}{[1+(8V-U)/2\pi]^{-1/2}} . \quad (49)$$

Finally, we can rewrite the Lagrangian

$$L=\tfrac{1}{2}(\partial_\mu\xi_{\text{CDW}})^2+\tfrac{1}{2}(D_\mu\xi_{\text{SDW}})^2+\frac{G_2}{a_0^2}\sum_\nu \cos(\beta_\nu\xi_\nu) + \frac{G_1}{2a_0^2}\cos(\beta_{\text{CDW}}\xi_{\text{CDW}})\cos(\beta_{\text{SDW}}\xi_{\text{SDW}}) , \quad (50)$$

$$D_0=\eta\partial_0 , \quad (51)$$

$$D_1=\frac{1}{\eta}\partial_1 . \quad (52)$$

Using the fact that operators of the form $\cos(\beta\phi)$ have dimension $\beta^2/4\pi$, we can read off the dimensions of the last three terms. The operators $\cos(\beta_{\text{CDW}}\xi_{\text{CDW}})$ and $\cos(\beta_{\text{SDW}}\xi_{\text{SDW}})$ have dimensions

$$\Delta_{1\mathrm{SDW}}=\frac{\beta_{\mathrm{SDW}}^2}{4\pi}=\frac{2}{[1+(12V+U)/2\pi]^{-1/2}(1+8V/2\pi)^{-1/2}}, \tag{53}$$

$$\Delta_{1\mathrm{CDW}}=\frac{\beta_{\mathrm{CDW}}^2}{4\pi}=\frac{2}{[1+(8V-U)/2\pi]^{-1/2}(1+8V/2\pi)^{-1/2}}. \tag{54}$$

Similarly, the term

$$\cos(\beta_{\mathrm{CDW}}\xi_{\mathrm{CDW}})\cos(\beta_{\mathrm{SDW}}\xi_{\mathrm{SDW}})$$

has dimension

$$\Delta_2=\frac{\beta_{\mathrm{CDW}}^2}{4\pi}+\frac{\beta_{\mathrm{SDW}}^2}{4\pi}+\Delta_{1\mathrm{CDW}}+\Delta_{1\mathrm{SDW}}. \tag{55}$$

The CDW-SDW phase boundary in our continuum model is the line $U=2V$. Along this line, at small values of the coupling constants, the dimension of Δ_1 is greater than 2, and therefore irrelevant. However, at a value $U\approx 1.45$ (in units of t), the operator is marginal and, above this value, becomes relevant, opening up a gap between the two CDW and SDW phases. Recalling that only the unklapp scattering term possesses a discrete symmetry, we can see that the phase transition associated with this operator becoming relevant is due to the increased importance of umklapp scattering.

It is also interesting to look at the scaling of the CDW order parameter:

$$m_{\mathrm{CDW}}=\sum_n(-1)^n C_n^\dagger C_n = \sum_{n,s}\sin(\pi n)C_{n,s}^\dagger C_{n,s}. \tag{56}$$

In terms of our field theory, this becomes

$$m=\sum_s \psi_{R,s}^\dagger\psi_{L,s}+\psi_{L,s}^\dagger\psi_{R,s} \tag{57}$$

$$=\sum_s \bar{\psi}\psi. \tag{58}$$

Transforming to Bose fields yields

$$m(x)=\sum_s\cos[\sqrt{4\pi}\phi_s(x)] \tag{59}$$

$$\begin{aligned}&=\cos\left[\frac{1}{\sqrt{2}}(\phi_{\mathrm{CDW}}+\phi_{\mathrm{SDW}})\right]\\&+\cos\left[\frac{1}{\sqrt{2}}(\phi_{\mathrm{CDW}}-\phi_{\mathrm{SDW}})\right]\\&=\cos[\sqrt{2\pi}\phi_{\mathrm{CDW}}(x)]\cos[\sqrt{2\pi}\phi_{\mathrm{SDW}}(x)]\\&=\cos\left[\frac{\beta_{\mathrm{CDW}}}{2}\xi_{\mathrm{CDW}}(x)\right]\cos\left[\frac{\beta_{\mathrm{SDW}}}{2}\xi_{\mathrm{SDW}}(x)\right].\end{aligned} \tag{60}$$

From this, we can obtain the CDW correlation function.

$$G(x,x')=\langle 0|Tm(x)m(x')|0\rangle_c$$

$$=\left\langle 0\left|T\cos\left[\frac{\beta_{\mathrm{CDW}}}{2}\xi_{\mathrm{CDW}}(x)\right]\cos\left[\frac{\beta_{\mathrm{SDW}}}{2}\xi_{\mathrm{SDW}}(x)\right]\cos\left[\frac{\beta_{\mathrm{CDW}}}{2}\xi_{\mathrm{CDW}}(x')\right]\cos\left[\frac{\beta_{\mathrm{SDW}}}{2}\xi_{\mathrm{SCW}}(x')\right]\right|0\right\rangle_c. \tag{61}$$

Along the critical line $U=2V$, this factorizes

$$\begin{aligned}G(x,x')&=\left\langle 0\left|T\cos\left[\frac{\beta_{\mathrm{CDW}}}{2}\xi_{\mathrm{CDW}}(x)\right]\cos\left[\frac{\beta_{\mathrm{CDW}}}{2}\xi_{\mathrm{CDW}}(x')\right]\right|0\right\rangle_c\\&\times\left\langle 0\left|T\cos\left[\frac{\beta_{\mathrm{SDW}}}{2}\xi_{\mathrm{SDW}}(x)\right]\cos\left[\frac{\beta_{\mathrm{SDW}}}{2}\xi_{\mathrm{SDW}}(x')\right]\right|0\right\rangle_c\\&=\left\langle 0\left|T\cos\left[\frac{\beta_{\mathrm{CDW}}}{2}\xi_{\mathrm{CDW}}(x)-\frac{\beta_{\mathrm{CDW}}}{2}\xi_{\mathrm{CDW}}(x')\right]\right|0\right\rangle_c\\&\times\left\langle 0\left|T\cos\left[\frac{\beta_{\mathrm{SDW}}}{2}\xi_{\mathrm{SDW}}(x)-\frac{\beta_{\mathrm{SDW}}}{2}\xi_{\mathrm{SDW}}(x')\right]\right|0\right\rangle_c.\end{aligned} \tag{62}$$

Thus the correlation function scales as $1/|x-x'|^{2D}$, and the dimension of the order parameter is

$$D=\frac{1}{4}\left[\frac{\beta_{\mathrm{CDW}}^2}{4\pi}+\frac{\beta_{\mathrm{SDW}}^2}{4\pi}\right]$$
$$=\frac{\Delta_2}{4}\ . \tag{63}$$

From this, we see that the exponent $\eta=2D-2+d$, will be one at the tricritical point, where D is exactly 2.

We can also find how the order parameter scales as the phase boundary is crossed. Away from the critical line the constant $G_2=(V-U/2)b/2\pi a_0^2$ will not be zero, and

$$m_{\mathrm{CDW}}\sim G_2[\cos(\beta_{\mathrm{CDW}}\xi_{\mathrm{CDW}})+\cos(\beta_{\mathrm{SDW}}\xi_{\mathrm{SDW}})]$$
$$\sim G_{2_{\mathrm{CDW}}}\cos(\beta_{\mathrm{CDW}}\xi_{\mathrm{CDW}})+G_{2_{\mathrm{SDW}}}\cos(\beta_{\mathrm{SDW}}\xi_{\mathrm{SDW}})\ . \tag{64}$$

Both operators will be strongly relevant below the tricritical point. The β function of the respective coupling constants will be

$$\beta(G_{2_{\mathrm{CDW,SDW}}})=\frac{\partial G_{2_{CDW,SDW}}}{\partial\ln(l)}$$
$$=(2-\Delta_{1_{\mathrm{CDW,SDW}}})G_{2_{\mathrm{CDW,SDW}}}$$
$$+O(G_{2_{\mathrm{CDW,SDW}}}^2)\ . \tag{65}$$

Thus the correlation lengths scale as

$$\xi_{\mathrm{CDW,SDW}}=|U-V/2|^{-\nu_{\mathrm{CDW,SDW}}}\ . \tag{66}$$

The dimension of m_{CDW} is

$$[m]=\frac{\Delta_2}{4}\ . \tag{67}$$

Thus

$$m\sim l^{-(1/4)(\Delta_{\mathrm{CDW}}+\Delta_{\mathrm{SDW}})} \tag{68}$$
$$\sim\xi_{\mathrm{CDW}}^{-(\Delta_{\mathrm{CDW}}/4)}\xi_{\mathrm{SDW}}^{-(\Delta_{\mathrm{SDW}}/4)}\ . \tag{69}$$

Substituting for the correlation lengths, this can be rewritten

$$m\approx|U-V/2|^{(1/4)(\nu_{\mathrm{CDW}}\Delta_{\mathrm{CDW}}+\nu_{\mathrm{SDW}}\Delta_{\mathrm{SDW}})}\ ,$$
$$m\approx|U-V/2|^{\beta}\ , \tag{70}$$
$$\beta=(\nu_{\mathrm{CDW}}\Delta_{\mathrm{CDW}}+\nu_{\mathrm{SDW}}\Delta_{\mathrm{SDW}})\ . \tag{71}$$

Expressing β in terms of the difference in the two scaling dimensions

$$\Delta_{\mathrm{CDW}}=\frac{(\Delta_{\mathrm{CDW}}+\Delta_{\mathrm{SDW}})}{2}+\delta\ , \tag{72}$$
$$\Delta_{\mathrm{SDW}}=\frac{(\Delta_{\mathrm{CDW}}+\Delta_{\mathrm{SDW}})}{2}-\delta\ , \tag{73}$$
$$\beta=\frac{1}{2}\frac{(1+\delta^2)}{(1-\delta^2)}\ . \tag{74}$$

Thus in the case where the two operators are symmetric $\delta\to0$, $\beta\to\frac{1}{2}$. At the tricritical point $\delta\approx0.1084$, and $\beta\approx0.512$.

III. CALCULATIONAL RESULTS

Our analysis, consistent with the argument of Hirsch,[7] has shown that the CDW-SDW transition should be second order for small values of the coupling constant and become first order as the coupling constant is increased. Furthermore, the gap in the fermionic spectrum, associated with the first-order transition, should exhibit Kosterlitz-Thouless scaling and disappear with an essential singularity at the tricritical point. We have performed Monte Carlo simulations to verify this phenomenon, and more accurately locate the position of the tricritical point. We performed the simulations using the world line method of Hirsch *et al.*[11] This is a quantum Monte Carlo technique which converts the one-dimensional quantum problem into a $(1+1)$-dimensional (space plus time) classical model which can be simulated by standard numerical approaches.

Our method for distinguishing between a first- or second-order transition is to measure the distribution of the CDW order parameter, and interpret this according to the phenomenological theory of Landau. This approach avoids some of the problems of measuring small values of a $Z(2)$ order parameter on a finite lattice. On a small finite lattice, there is a high probability of transitions between the "up" and "down" phases (corresponding in this case to CDW's on odd or even sites), and any averaged estimate of the order parameter will tend toward zero. Conversely, use of the absolute value or square of the order parameter as an estimator will always indicate the presence of order, even in the case where there is no order. In fact, if the order parameter is actually zero, this method simply estimates the standard deviation of the distribution.

Measurement of the actual distribution avoids these problems. Following Landau, we assume that in the thermodynamic limit the order parameter will occur at the value where the free energy is a minimum (i.e., the maximum of the measured distribution). If the maximum of the distribution changes discontinuously as the phase boundary is crossed, then there will be a first-order transition marked by a discontinuous change of the order parameter in the thermodynamic limit.

Figure 3 shows an example of the probability distribu-

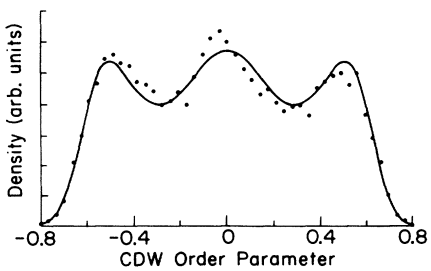

FIG. 3. Density function of the CDW order parameter measured during simulation of 24×24 lattice ($\beta=6.0$). $U=2.284$, $V=1.222$.

tion function of the CDW order parameter measured near the phase boundary where $U \approx 2.28$. The solid line is least-squares fit of the function

$$f(x) = A \exp\left[\sum_i a_{2i} x^{2i}\right] . \quad (75)$$

The first was obtained by applying a polynomial fitting routine to the logarithm of the measured data. This and other simulations shown here were performed on a 24-site lattice with 24 time slices. β was 6.0. Thus $\Delta\tau$ defined on the lattice was 0.25 ($\Delta\tau_{\text{physical}} = 2\Delta\tau_{\text{lattice}} = 0.5$). Each calculation at a particular value of U and V consisted of 45 000 Monte Carlo sweeps following 15 000 sweeps for thermalization. Measurements were performed after every five sweeps.

Several things should be noted about this plot. First, and most important, is the presence of metastable states, indicated by the unequal maxima. As the coupling constants vary in the direction of the CDW region (increasing V, and decreasing U) the probability of finding the system in one of the outer (nonzero) states will increase until at the transition there is a discontinuous change in the position of the maximum of the distribution. Thus, in the thermodynamic limit there will be a first-order transition manifested by a discontinuous change in the order parameter. This behavior is shown in the three-dimensional plot of Fig. 4, generated from a sequence of these calculations, crossing the phase boundary near $U = 2.28$. The values of the coupling constants for each step of the calculation are listed in Table I. Each constant U rib appearing in the plot is a curve fit to the probability density function measured from a Monte Carlo calculation in the same manner as Fig. 3. From this graph the discontinuous change in the maximum of the distribution when moving from the SDW ($m_{\text{CDW}} = 0$) to the CDW phase is obvious. Note that the value of $U \approx 2.28$ is well below the position of the tricritical point estimated by Hirsch ($U = 3.0$), and that the position of the phase boundary of approximately $U = 2.284, V = 1.222$ is shifted from the $U = 2V$ line as found by Hirsch, and by Fourcade and Spronken.

TABLE I. U and V values used for the calculations shown in Figs. 4 and 5.

Figure 4		Figure 5	
U	V	U	V
2.288	1.214	0.805	0.490
2.286	1.218	0.800	0.500
2.284	1.222	0.795	0.510
2.280	1.230	0.785	0.520
2.278	1.234	0.780	0.540
2.276	1.238	0.775	0.550
2.274	1.242	0.770	0.560

It is also interesting to see from Fig. 3, why the hysteresis normally associated with a first-order transition was not observed in these simulations. Hysteresis occurs in crossing a phase boundary when a physical system becomes temporarily trapped in a metastable state. However, from the relative symmetry in the experimental data, it is clear that the frequency of tunneling between the various metastable and ground states was high relative to the period of the Monte Carlo measurement. Thus, for the value of the coupling constants, lattice size, and Monte Carlo run times at which these measurements were made, the system was not trapped in the metastable states, and hysteresis is unlikely to be observed.

In contrast to the first-order transition shown in Figs. 3 and 4, a transition that appears to be second order is shown in Fig. 5. This figure displays the results of a sequence of measurements crossing the phase boundary near $U = 0.8$. There is no indication of any metastable states, and the order parameter changes continuously from zero to a nonzero value at the phase boundary. Because the gap associated with the first-order transition is thought to disappear slowly, it is impossible to rule out the possibility of a weak first-order transition in this case.

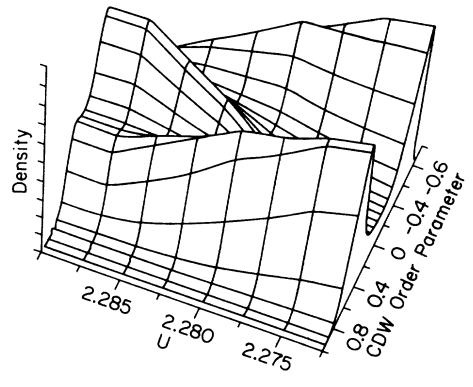

FIG. 4. Variation of the CDW order parameter as the CDW-SDW phase boundary is crossed near $U = 2.28$. Note the discontinuous change in the position of the maximum, signaling a first-order transition. The series of measurements used to produce this figure were made on a 24×24 site lattice with $\beta = 4.0$. The values of U and V used in the calculations are shown in Table I.

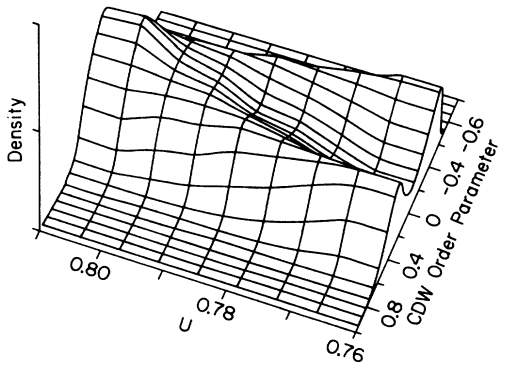

FIG. 5. Variation of the CDW order parameter as the CDW-SDW phase boundary is crossed near $U = 0.8$. Note the continuous change in the position of the maximum, signaling a second-order transition. The series of measurements used to produce this figure were made on a 24×24 site lattice with $\beta = 4.0$. The values of U and V used in the calculations are shown in Table I.

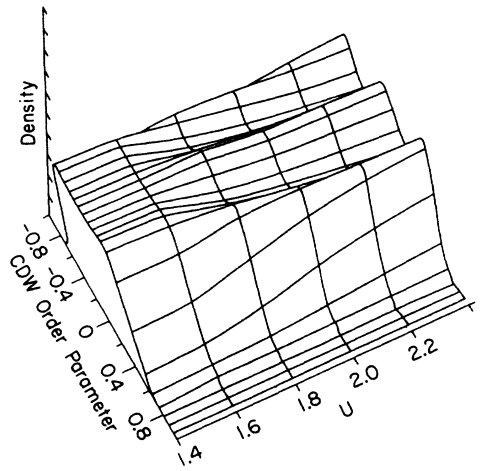

FIG. 6. Variation of the CDW order parameter along the CDW-SDW phase boundary. The three maximum characteristic of a first-order transition appear at approximately $U=1.5$. The values of U and V used in the calculations for this figure are shown in Table II.

Once again, the shifted phase boundary is observed.

Figure 6 shows the change in the probability distribution of CDW order parameter versus position along the phase boundary. The triple minima characteristic of a first-order transition disappear around $U=1.6$. Based on this figure, and the knowledge that the gap associated with the transition appears very slowly, we estimate the tricritical point to occur at roughly $U=1.5\pm0.1$ in units of t. This number is lower than the value of 3.0 found by Hirsch.[8] However, we believe this difference may be due to a difference in the respective energy scales resulting from the fact that Hirsch used the lattice $\Delta\tau$ rather than the physical $\Delta\tau$ ($=2\Delta\tau_{\text{lattice}}$) to calculate the matrix elements for his simulations. Of course, to estimate more accurately the position of the tricritical point, it is necessary to use finite-sized scaling to extrapolate to the thermodynamic limit. However, based on the calculations we performed on lattice sizes of 16 and 36 sites, we expect the change in the position of the tricritical point when extrapolated to the thermodynamic limit to be of the same order as the uncertainty here in estimating the point's position.

The U value of the tricritical point agrees surprisingly well with the value found in Sec. I. This may be fortuitous, considering the uncertainty in approximating the lattice by a continuum model, particularly in the case when the charged- and spin-density waves in which we are interested have a period on the order of the lattice constant.

In addition to these calculations, we attempted to measure the value of η, and the value of the conformal anomaly. However, the checkerboard approach does not yield sufficiently accurate data for these measurements. Measurement of η is hampered by the fact that for finite sizes the disconnected piece of the CDW correlation function is very large, and there is a periodic fluctuation in the correlation functions that is apparently an artifact of the checkerboard breakup. These factors make it difficult to estimate the decay constant reliably. Measurement of the conformal anomaly using Monte Carlo methods requires a more accurate estimate of energy than could be obtained with the computer time available to us. Results of calculations of the conformal anomaly using Lancoz methods along the critical line will be published.[12]

TABLE II. U and V values used for the calculations shown in Fig. 6.

Figure 6	
U	V
2.2840	1.2220
2.1411	1.1522
1.9982	1.0825
1.8552	1.0128
1.7123	0.9430
1.5694	0.8732

IV. CONCLUSION

We have studied the phase diagram of the extended Hubbard model at half-filling analytically in the continuum limit, and shown that umklapp scattering underlies the tricritical behavior. In addition, we have calculated the critical exponents along the critical line. Finally, using Monte Carlo simulations, we have estimated the tricritical point to occur at approximately $U=1.5$ in units of t. Our simulations confirm the shift of the CDW-SDW phase boundary away from $U=2V$ towards the CDW region.

Our method of Bosonization does not retain the full symmetry of the Hamiltonian. It would be interesting to see what differences would be found using more sophisticated non-Abelian methods of converting from Bose to Fermi fields,[13] which preserve the symmetry.

ACKNOWLEDGMENTS

This work was supported in part by National Science Foundation (NSF) Grant Nos. DMR 88-18713 and DMR 86-12860/24. We would like to thank the staff of the University of Illinois Materials Research Laboratory Center for Computation for their assistance. The calculations were performed on the center's FPS-164 array processor.

[1]V. J. Emery, in *Highly Conducting One-Dimensional Solids*, edited by J. T. Devreese, R. P. Evrard, and V. E. van Doren (Plenum, New York, 1979).
[2]D. Cabib and E. Callen, Phys. Rev. B **12**, 5249 (1975).
[3]B. Fourcade and G. Spronken, Phys. Rev. B **29**, 5089 (1984).
[4]B. Fourcade and G. Spronken, Phys. Rev. B **29**, 5096 (1984).
[5]L. Sneddon, J. Phys. C **11**, 2823 (1975).
[6]B. Nienhuis, A. N. Berker, E. K. Riedel, and M. Schick, Phys.

Rev. Lett. **43**, 737 (1979).
[7]J. E. Hirsch, Phys. Rev. B **31**, 6022 (1985).
[8]J. E. Hirsch, Phys. Rev. Lett. **53**, 2327 (1984).
[9]S. Mandelstam, Phys. Rev. D **11**, 3026 (1975).
[10]E. Witten, Nucl. Phys. **B142**, 285 (1978).
[11]J. E. Hirsch, D. J. Scalapino, R. L. Sugar, and R. Blankenbecler, Phys. Rev. B **26**, 5033 (1982).
[12]R. T. Scalettar and J. W. Cannon (unpublished).
[13]E. Witten, Commun. Math. Phys. **92**, 4 (1984); **92**, 455 (1984).